SUPPLEMENTARY FIGURES

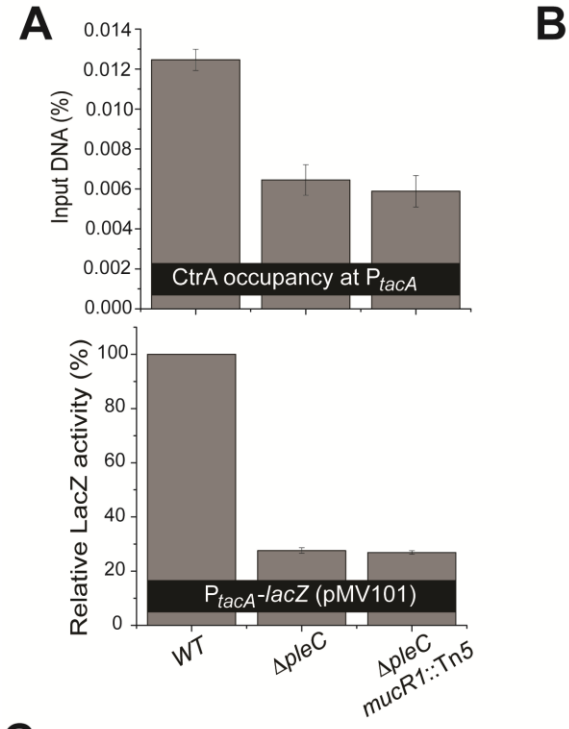

B

P_*lacZ* activity (% *WT*) of CtrA ChIP-Seq targets

P_*lacZ* \ Strain	*WT*	Δ*pleC*
flaF	100.7 ± 1.0	57.9 ± 4.9
fljM	105.4 ± 7.7	40.7 ± 7.5
perP	102.3 ± 3.3	32.8 ± 7.8
pilA	99.1 ± 1.3	25.6 ± 5.9
pilA(synUTR)	100.0 ± 3.6	14.2 ± 1.1
sciP	98.9 ± 1.6	25.2 ± 2.3
CC_0095 (hfsJ)	99.3 ± 1.8	14.8 ± 3.3
CC_0845	95.1 ± 5.6	35.8 ± 1.0
CC_1101	102.4 ± 4.5	45.8 ± 3.2
CC_1128	104.1 ± 5.6	17.5 ± 1.6
CC_1697	104.5 ± 6.9	20.6 ± 1.5
CC_1982	101.0 ± 2.7	23.9 ± 1.6
CC_1999	102.7 ± 3.1	26.9 ± 2.5
CC_2199	96.5 ± 5.0	16.7 ± 0.7
CC_2324	97.9 ± 3.5	25.3 ± 3.4
CC_2839	99.1 ± 4.3	21.8 ± 2.7
CC_2882	98.9 ± 1.9	49.7 ± 1.2
CC_2939	97.1 ± 5.1	21.2 ± 4.1
CC_3144	99.3 ± 1.2	62.7 ± 2.7
CC_3689	100.6 ± 1.4	57.5 ± 5.6

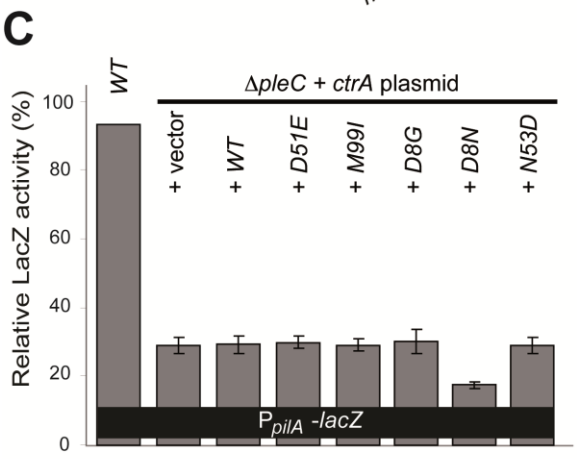

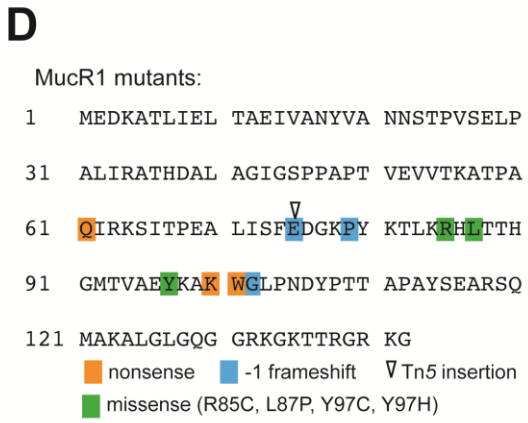

Supplementary Figure 1 *tacA* transcription is PleC-dependent, but not MucR-dependent. **A.** Transcription of *tacA* expression is PleC-dependent, but is not affected by *mucR1*::Tn*5*. qChIP followed at P$_{tacA}$ in WT, Δ*pleC* and Δ*pleC mucR1*::Tn*5* using antibodies to CtrA. Error is shown as S.D.. **B**. Promoter-probe assays using CtrA-bound promoters and *lacZ* in WT and in Δ*pleC*. All these promoters presented an altered CtrA binding in Δ*pleC* and their transcription is also affected in Δ*pleC* cells. The *pilA(synUTR)*-reporter is a modified version of *pilA* in which the 74 nt untranslated region (UTR) has been replaced by a synthetic UTR from *E. coli* expression vector pET28a (see Supplementary Note 1 for sequence). Error is shown as S.D.. **C.** *β*-galactosidase activity measured in promoter-probe plasmid harboring the P*pilA* promoter fused to *lacZ* (P*pilA-lacZ*) in WT and in Δ*pleC* carrying different CckA-independent phosphomimetic variants of *ctrA* that we isolated *(*see *Methods)*. Neither can restore *pilA* expression. Error is shown as S.D.. **D**. Map of the *mucR1* mutations that restore kanamycin resistance and *pilA* expression to Δ*pleC* Δ*mucR1 pilA*::P$_{pilA}$-*nptII* cells. The black arrow indicates the Tn*5* insertion.

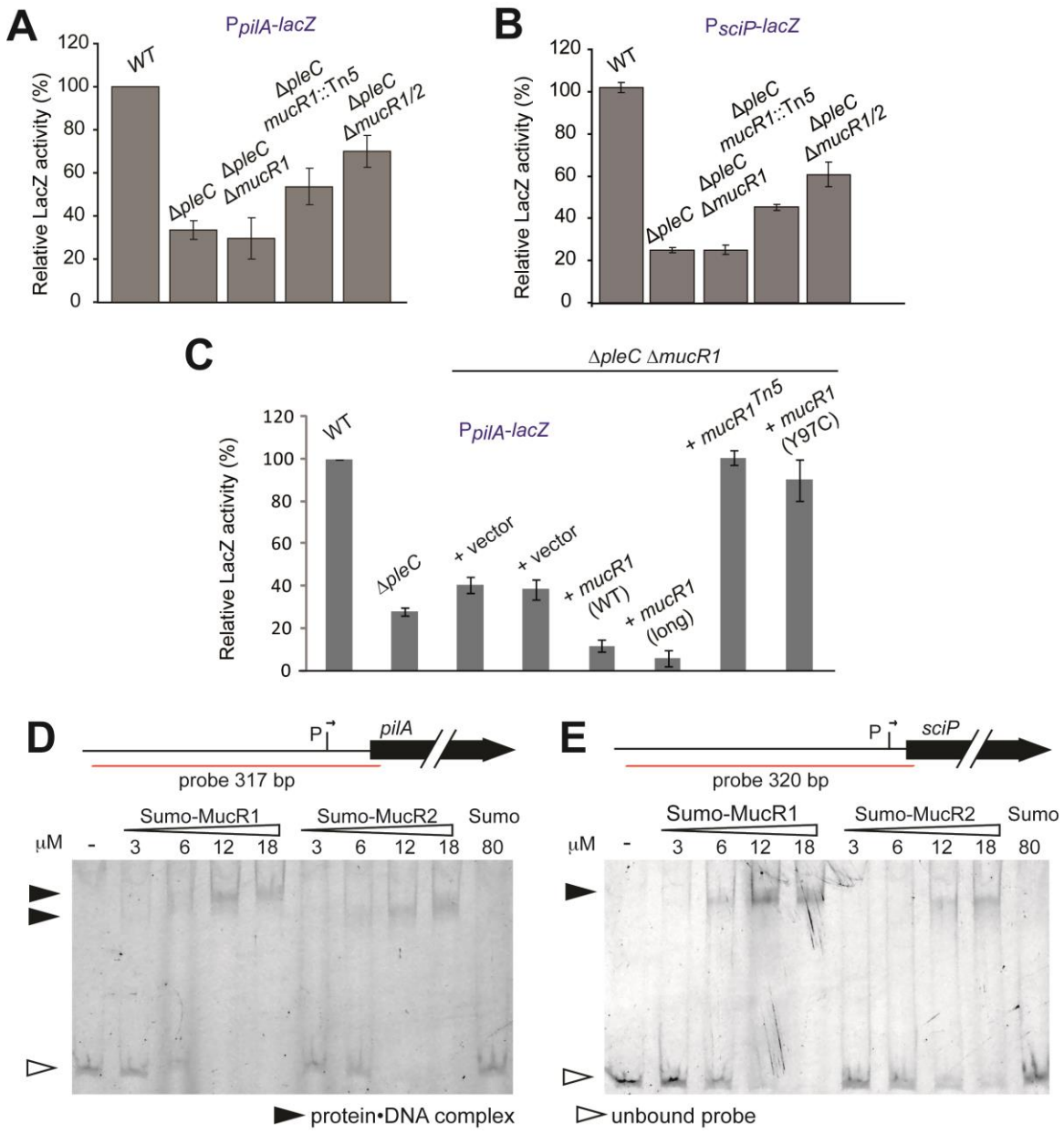

Supplementary Figure 2. Direct binding of MucR1 and MucR2 to P_{pilA} and P_{sciP}.
A-C. Promoter-probe assays of transcriptional reporters carrying the *pilA*(A) or *sciP* (B) promoter fused to *lacZ,* measured in WT, Δ*pleC*, Δ*pleC* Δ*mucR1* double mutant Δ*pleC mucR1*::Tn*5* double mutant and Δ*pleC* Δ*mucR1* Δ*mucR2* triple mutant cells. Panel C shows promoter probe assays of P_{pilA}-*lacZ* conducted in Δ*pleC* Δ*mucR1* double mutant cells harboring various pMT335-derived plasmids. Error is shown as S.D.. **D-E.** Electrophoretic Mobility Shift Assay (EMSA) showing that purified N-terminally His_6-SUMO-tagged MucR1 or -MucR2, but not His_6-SUMO alone, binds fluorescently-labeled P_{pilA} (C) and P_{sciP} (D) probes *in vitro*. His_6-SUMO alone does not bind either probe. The white arrows indicate the unbound probes.

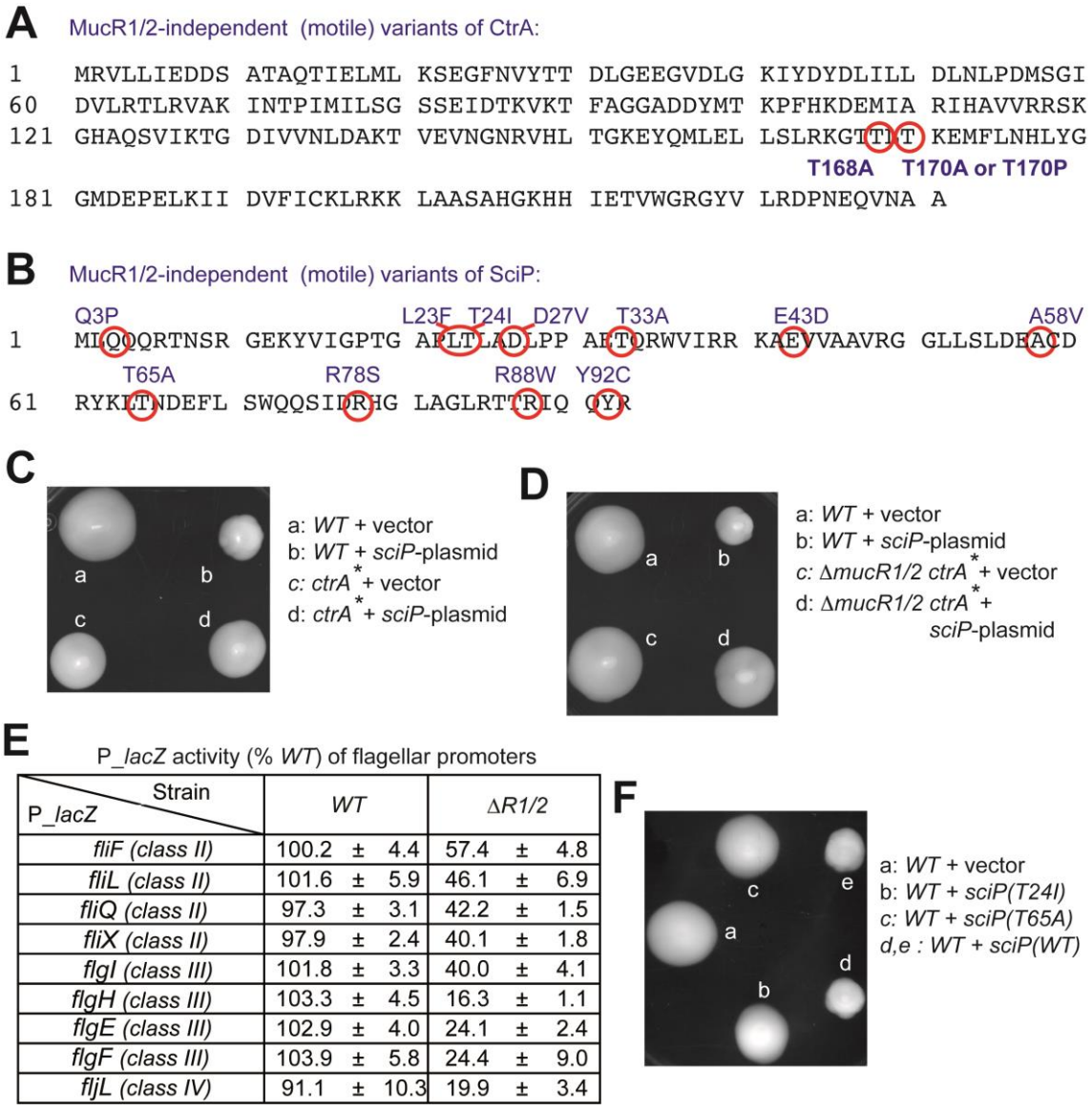

P_lacZ \ Strain	WT	ΔR1/2
fliF (class II)	100.2 ± 4.4	57.4 ± 4.8
fliL (class II)	101.6 ± 5.9	46.1 ± 6.9
fliQ (class II)	97.3 ± 3.1	42.2 ± 1.5
fliX (class II)	97.9 ± 2.4	40.1 ± 1.8
flgI (class III)	101.8 ± 3.3	40.0 ± 4.1
flgH (class III)	103.3 ± 4.5	16.3 ± 1.1
flgE (class III)	102.9 ± 4.0	24.1 ± 2.4
flgF (class III)	103.9 ± 5.8	24.4 ± 9.0
fljL (class IV)	91.1 ± 10.3	19.9 ± 3.4

Supplementary Figure 3 Mutations in SciP or CtrA suppress the motility defect of Δ*mucR1/2* cells. A-B. Position of the different point mutations in *ctrA* (A) and *sciP* (B) that restore motility to Δ*mucR1/2* (Δ*R1/2*) cells. **C.** The *ctrA** mutation renders WT cells insensitive to motility inhibition by mild *sciP* over-expression from pMT335 (in the absence of inducer). Swarm (0.3%) agar was inoculated with the different strains. **D.** The *ctrA** mutation renders Δ*R1/2* cells insensitive to motility inhibition by mild *sciP* over-expression from pMT335 (in the absence of inducer). Swarm agar was inoculated with the different strains. **E.** Promoter-probe assays of transcriptional reporters carrying flagellar promoters fused to *lacZ* in WT and Δ*R1/2*. The expression of all classes of flagellar genes (II, III and IV) are affected by the Δ*mucR1* Δ*mucR2* double deletion. Error is shown as S.D.. **F**. Mild over-expression of WT but not the hypomorphic *sciP* alleles from pMT335 (in the absence of inducer) impairs motility in WT cells on motility (0.3%) agar.

A

P_*lacZ* activity (% *WT*) of **SciP** ChIP-Seq targets

P_*lacZ* / Strain	*pleA*	*flgB*	*CC_3439*	*CC_3676*
WT	103.1 ± 6.9	100.0 ± 5.9	103.5 ± 8.9	107.9 ± 14.1
ΔR1/R2	31.2 ± 6.8	18.9 ± 2.2	38.6 ± 5.5	31.5 ± 4.7
*ΔR1/R2 sciP**	51.4 ± 8.0	54.1 ± 10.9	70.8 ± 9.1	54.3 ± 3.3
*ΔR1/R2 ctrA**	60.4 ± 11.6	74.9 ± 10.7	77.4 ± 5.4	58.5 ± 1.7

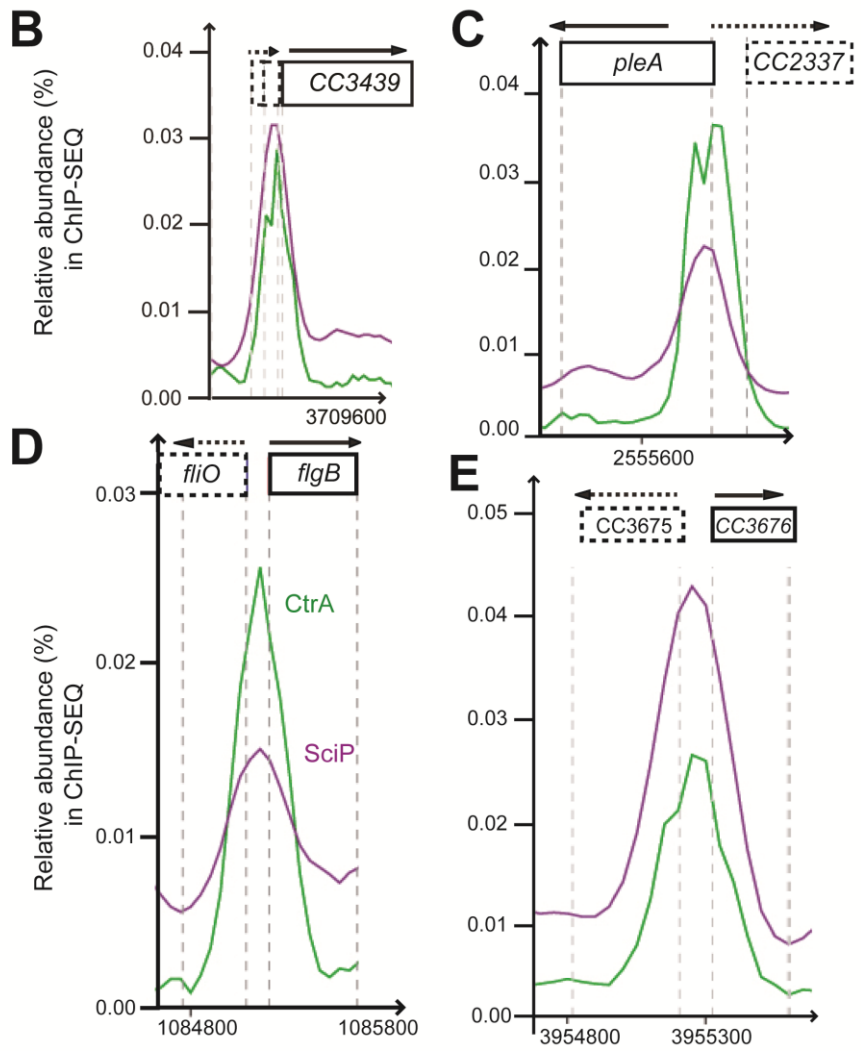

Supplementary Figure 4. SciP-bound promoters are poorly active in Δ*R1/2* cells.
A. Promoter-probe assays using various transcriptional reporter plasmids carrying SciP-target promoters in WT, Δ*R1/2*, in Δ*R1/2 sciP** and Δ*R1/2 ctrA** cells. Error is shown as S.D.. **B-E.** Traces of the occupancy of CtrA (green) and SciP (purple) at the promoters of *CC_3439* (B), *pleA* (C), *flgB* (D) and *CC_3676* (E) as determined by ChIP-Seq.

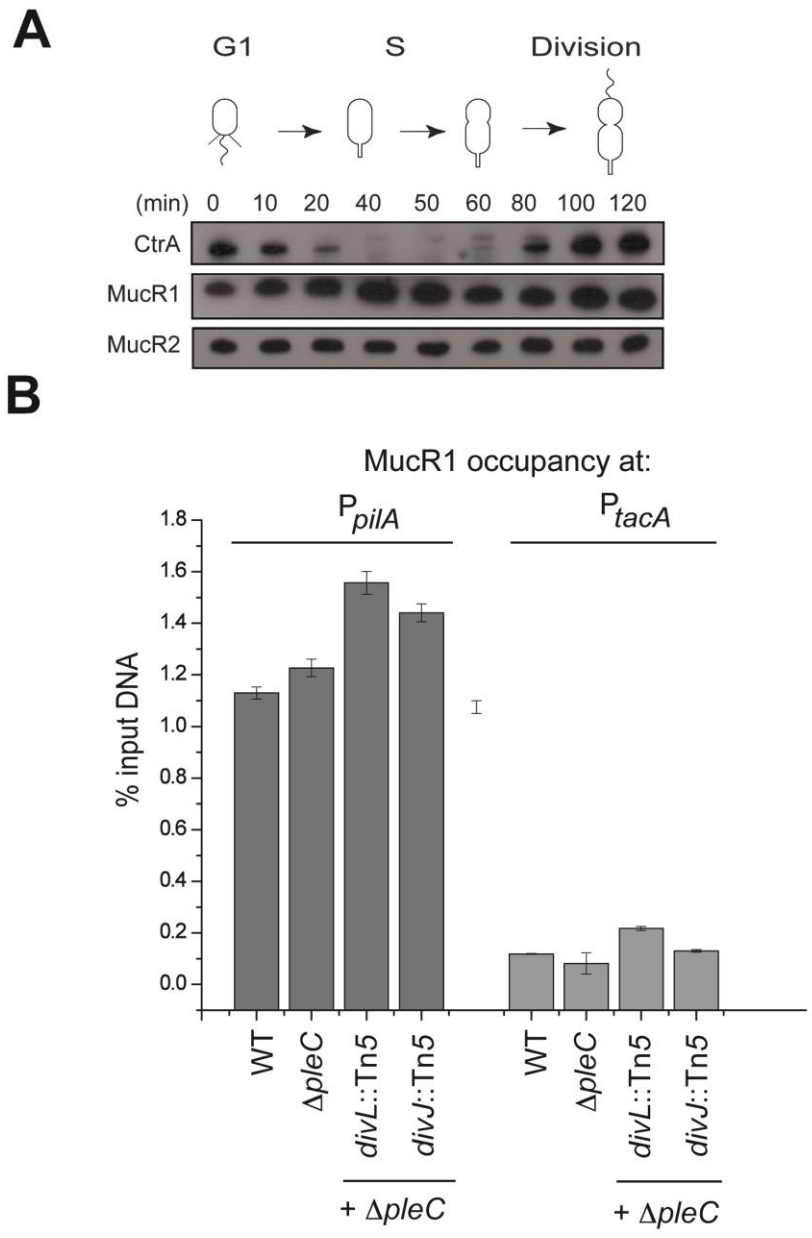

Supplementary Figure 5. Regulation of MucR1 binding by cell cycle kinases.
A. Immunoblots showing CtrA, MucR1 and MucR2 levels during cell cycle using polyclonal antibodies raised against MucR1, MucR2 or CtrA. **B**. MucR1 occupancy at P_{pilA} and P_{tacA} in WT and mutant cells as determined by qChIP. P_{tacA} occupancy is monitored as negative control. Error is shown as S.D..

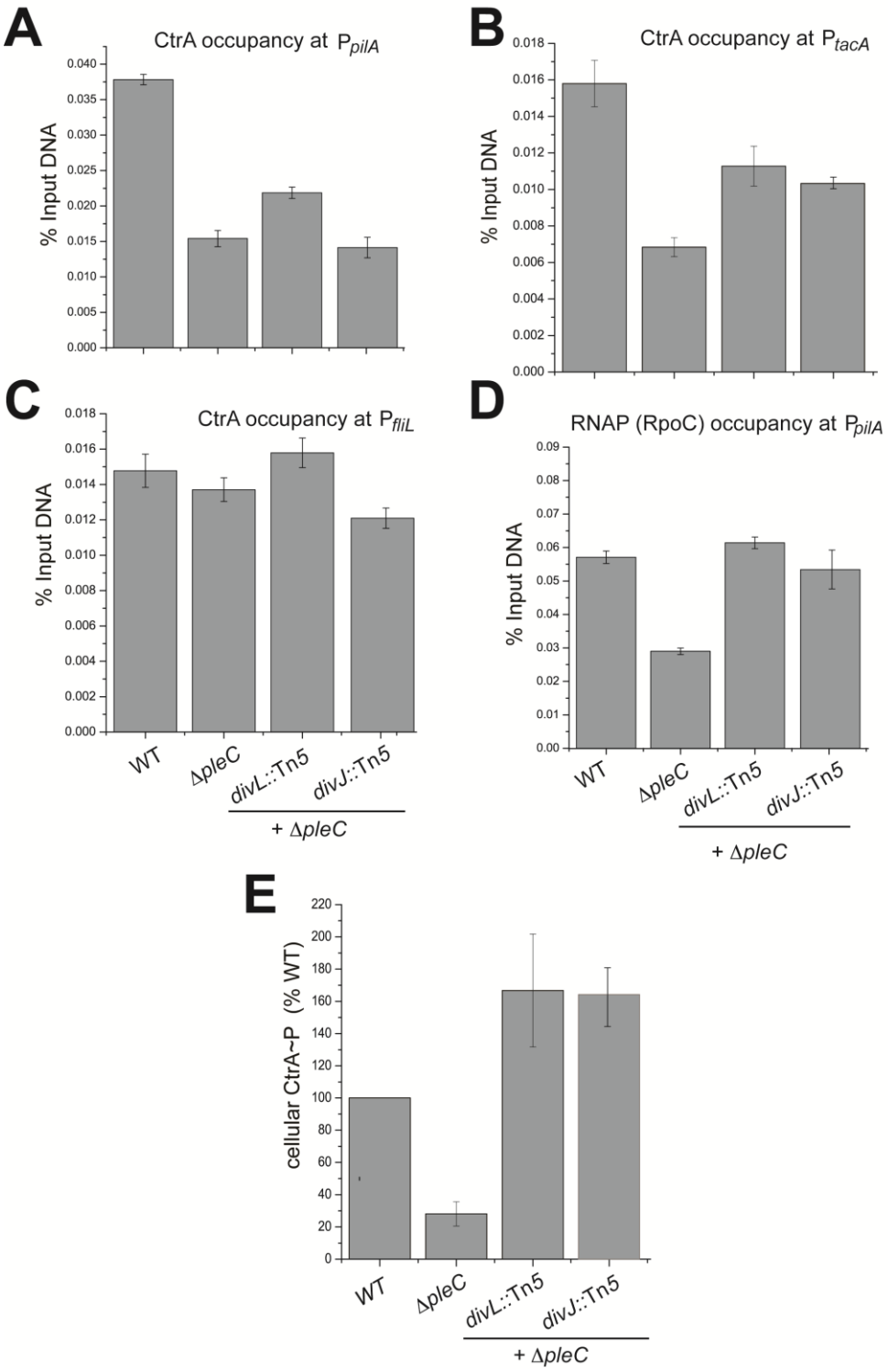

Supplementary Figure 6. CtrA occupancy and phosphorylation in WT and Δ*pleC* derivatives. A-D. Occupancy of CtrA (**A-C**) and RNA polymerase (RNAP, **D**) at P_{pilA} (**A, D**), P_{tacA} (**B**) and P_{fliL} (**C**) in WT and Δ*pleC* mutant derivatives as determined by qChIP using antibodies to CtrA and the RpoC subunit of RNAP. Error is shown as S.D..**E.** CtrA~P levels in WT and Δ*pleC* mutant were determined by P^{32} labeling followed by immunoprecipitations using antibodies to CtrA [18]. Error is shown as S.D..

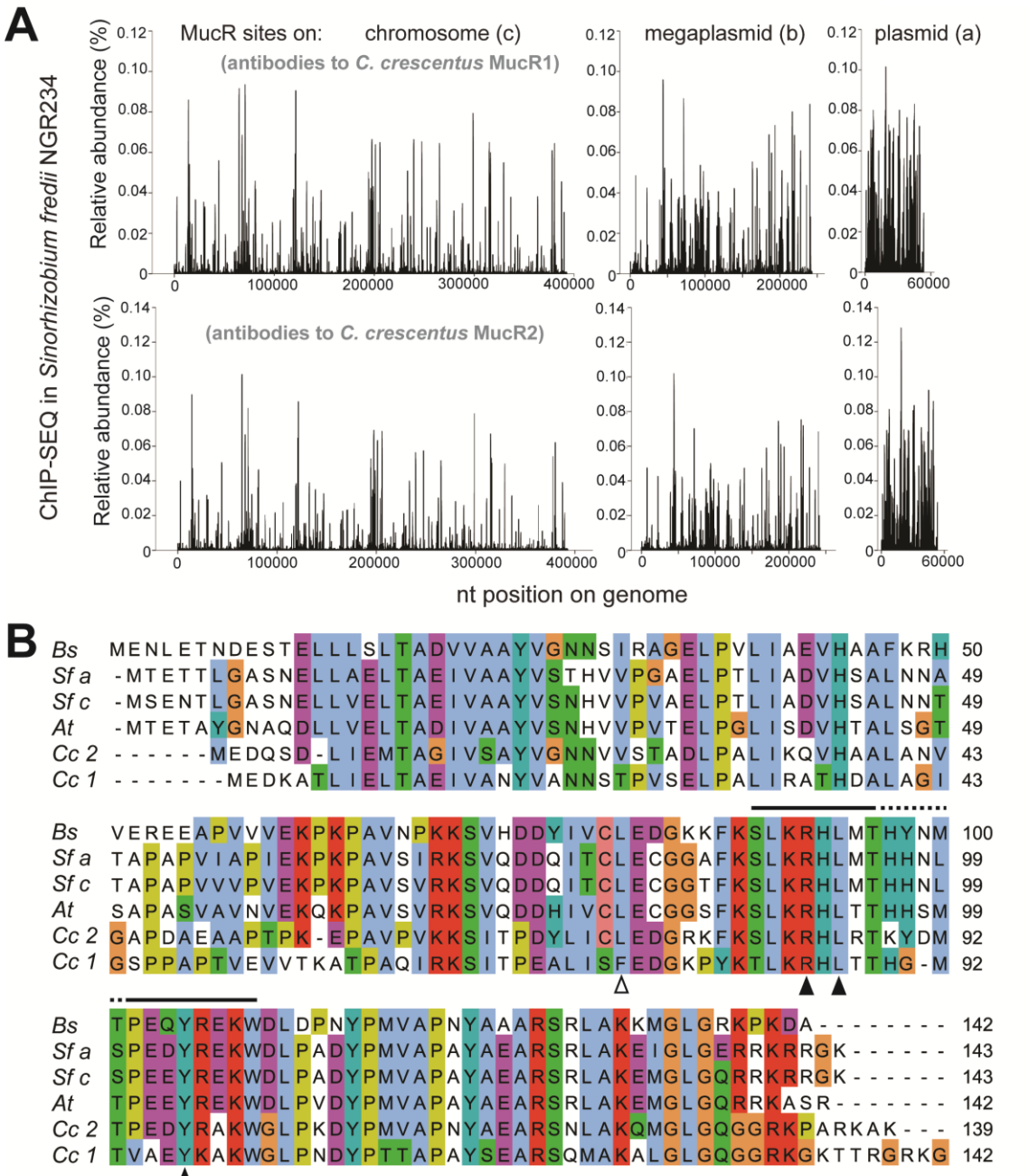

Supplementary Figure 7. Genome-wide occupancy of MucR on the genome of *Sinorhizobium fredii*. A. Genome-wide occupancy of MucR in *S. fredii* NGR234 as determined by ChIP-Seq using antibodies to *C. crescentus* MucR1 (upper panel) or MucR2 (lower panel). The *x*-axis represents the nucleotide position on the genome. Based on the nearly congruent binding profiles across the 3.9 Mbp *S. fredii* chromosome (c), the 2.4 Mbp megaplasmid pNGR234b (b) and the 0.5 Mbp symbiotic plasmid pNGR234a (a), it appears that the *c07580* and *a00320* gene products target the same promoters or that the two antibodies precipitated the same MucR homologue of *S. fredii*. **B.** Alignment of MucR homologues. The black line highlights two conserved alpha-helices of MucR/Ros from *Agrobacterium tumefaciens*, with the first one harboring residues contacting DNA. The white arrowhead indicates the site of the Tn*5* insertion in *C. crescentus mucR1*. The black arrows denote the different MucR21 missense mutations that restore *pilA* transcription to Δ*pleC* Δ*mucR1* cells, through trans-dominance on *mucR2* (also shown in Supplementary Figure 1D).

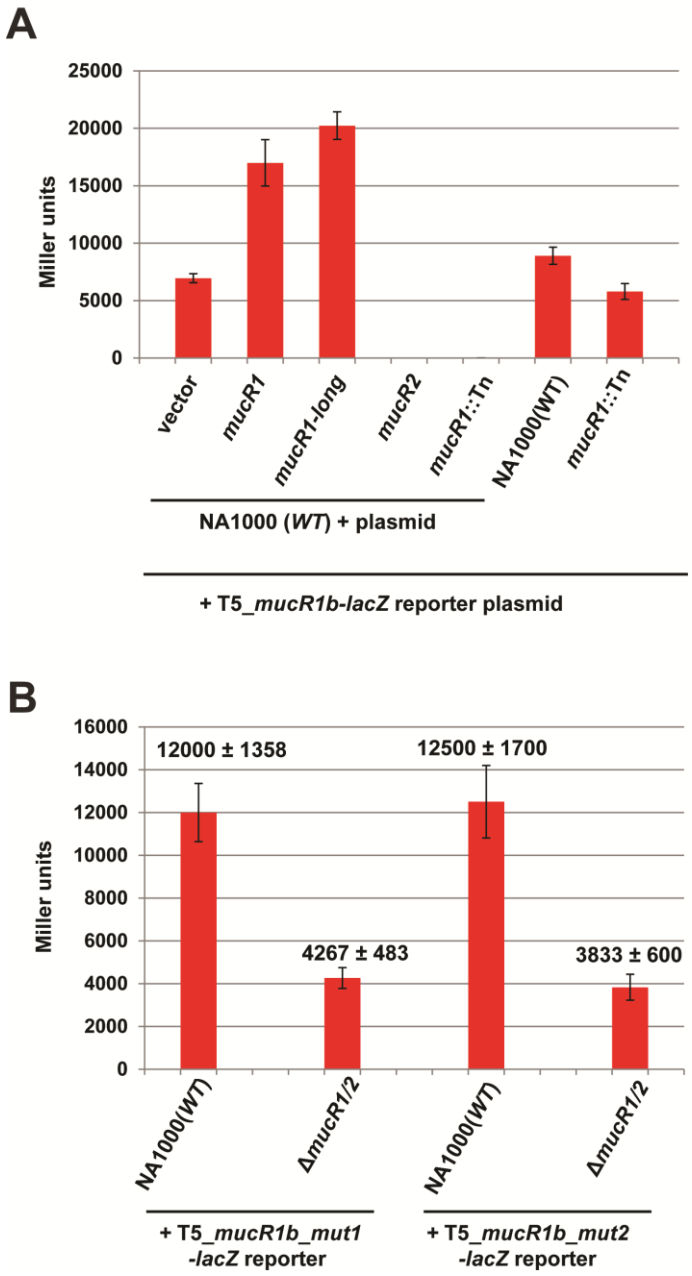

Supplementary Figure 8. The MucR1 consensus sequence is sufficient to confer MucR-dependent transcriptional control. **A**. Promoter-probe assays of transcriptional reporters carrying the T5_*mucR1b* synthetic promoter (T5 promoter followed by two putative MucR1 binding sites) fused to *lacZ*, measured in wild-type NA1000 cells overexpressing MucR1, MucR1-long, MucR2 and MucR::*Tn*. The two columns on the right show the β-galactosidase activity (expressed as Miller Units) in NA1000 wild-type and in the *mucR1*::Tn*5* strain. Error is shown as S.D..**B**. Promoter-probe assays of transcriptional reporters carrying two attenuated versions of the T5_mucR1b promoter (*mut1* and *mut2*, each harboring a point mutation in the predicted -10 or the -35 region of the T5 promoter, respectively, see Supplementary Note 1) fused to *lacZ* measured in wild-type NA1000 and Δ*mucR1*Δ*mucR2* cells. Error is shown as S.D.. Values are shown in Miller Units. Note that MucR1 acts positively on these reporters while MucR2 has a negative effect, presumably due to heterodimer formation (see Figure 4A).

SUPPLEMENTARY TABLES

Supplementary Table 1: List of oligonucleotides used in this study.

Oligo	Sequence
P_*CC_0095 (hfsJ/CCNA_00094)*	5'-AAA AAA GAA TTC ACC CCA AGG GCC ACG CCC AGA A-3'
P_*CC_0095 (hfsJ/CCNA_00094)*	5'- AAA AAA TCT AGA GGC CCA CCA GGC GCG CCC AGA A-3'
P_*CC_0168 (CCNA_00167)*	5'- AAA AAA GAA TTC CCC TGG CGG CTC TGG GGA CCT A-3'
P_*CC_0168 (CCNA_00167)*	5'- AAA AAA TCT AGA AGC AGG TCC AGG CGC CCA TGA A-3'
P_*CC_0420 (CCNA_00425)*	5'- AAA AAA GGA TCC TGT CCA GGT CAC TCA AGG A-3'
P_*CC_0420 (CCNA_00425)*	5'- AAA AAA AAG CTT ACT ATA TAC ATC AGT CTC ACC ATA-3'
P_*CC_0429 (CCNA_00438)*	5'- AAA AAA AGA TCT GAT GTT CGA GAT GCG CTT GGA AA-3'
P_*CC_0429 (CCNA_00438)*	5'- AAA AAA AAG CTT AAC GGG CCA TTT GAT CTT CGA AA-3'
P_*CC_0430 (CCNA_00439)*	5'- AAA AAA AGA TCT GTC CAC GAC CTT GCA GTC CGA CA-3'
P_*CC_0430 (CCNA_00439)*	5'- AAA AAA AAG CTT GCC ATC ACG GCC AGC ATC AGA A-3'
P_*CC_0591 (CCNA_00628)*	5'- AAA AAA GAA TTC AGC TCG AAC ATC GAC CGT CCC TTT T-3'
P_*CC_0591 (CCNA_00628)*	5'- AAA AAA ACT AGT TCT TGT AGT CGT CGA CGA CGA GGA-3'
P_*CC_0593 (CCNA_00629)*	5'- AAA AAA GAA TTC TTG TAG TCG TCG ACG ACG AGG A-3'
P_*CC_0593 (CCNA_00629)*	5'- AAA AAA ACT AGT AGC TCG AAC ATC GAC CGT CCC TTT T-3'
P_*fljM (CC_0792, CCNA_00834)*	5'- AAA AAA GAA TTC ATC CGG CGC TCG CCG GTC ACT CA-3'
P_*fljM (CC_0792, CCNA_00834)*	5'- AAA AAA TCT AGA ACT GGT TCT TGG CGG TCG CCC AGA-3'
P_*CC_0845 (CCNA_00888)*	5'- AAA AAA GAA TTC ATG GGC GAT GCG GTC ATC GAG GAA-3'
P_*CC_0845 (CCNA_00888)*	5'- AAA AAA TCT AGA CGA TCA TGT CGG CGG CGC GCT GGA A-3'
P_*sciP* (*CC_0903,CCNA_00948*)	5'- AAA AAA GAA TTC ATC GCC ACC TTC TCG AAC CCC AA-3'
P_*sciP* (*CC_0903,CCNA_00948*)	5'- AAA AAA AAG CTT GCG AGA GCA GAC CCC CGC GAA-3'
P_*mucR1* (*CC_0933,CCNA_00982*)	5'- AAA AAA GAA TTC GAT GTG GCC GTC GCC TGA CCT T-3'
P_*mucR1* (*CC_0933,CCNA_00982*)	5'- AAA AAA AAG CTT GGC GTA GCC TTG GTC ACC ACT T-3'
P_*mucR2* (*CC_0949, CCNA_00998*)	5'- AAA AAA GAA TTC ATC GCA CCG GCG CCA CCG ACC CGA A-3'
P_*mucR2* (*CC_0949, CCNA_00998*)	5'- AAA AAA TCT AGA CGC GGC GTG AAC CTG CTT GAT CAA-3'
P_*CC_1101 (CCNA_01157)*	5'- AAA AAA CAA TTG AGG CCG GCG CCG ATC CGA AGG AAA-3'
P_*CC_1101 (CCNA_01157)*	5'- AAA AAA TCT AGA ATA GGC GTA GAA CTT CTC GCG GTA A-3'
P_*CC_1128 (CCNA_01186)*	5'- AAA AAA GAA TTC GAA AGG TTC AGA TCG CCG ACC TTG A-3'
P_*CC_1128 (CCNA_01186)*	5'- AAA AAA TCT AGA TTT CGG CGA TGC ACA TCG CGG CCT T-3'
P_*CC_1697 (CCNA_01768)*	5'- AAA AAA GAA TTC AGC GCG CCA AGC AGG CCG TGA AA-3'
P_*CC_1697 (CCNA_01768)*	5'- AAA AAA TCT AGA CGA GCG GCC CAC CTC GAC GTC GAA-3'
P_*CC_1982 (CCNA_02061)*	5'- AAA AAA GAA TTC AGG ACG CCG ACA CCC AGC ATG A-3'
P_*CC_1982 (CCNA_02061)*	5'- AAA AAA TCT AGA TCG CTC TCG GAG ATG CGA GCG CGA A-3'
P_*CC_1999 (CCNA_02078)*	5'- AAA AAA GAA TTC GCG CCC TTC ACA AGC ATG CGA A-3'
P_*CC_1999 (CCNA_02078)*	5'- AAA AAA TCT AGA ACG GCT CCG GCG GTC GCC AGC AAC A-3'
P_*CC_2199 (CCNA_02282)*	5'- AAA AAA GAA TTC CGT CGA TCT GGT GCT GAC CTG GAA-3'
P_*CC_2199 (CCNA_02282)*	5'- AAA AAA TCT AGA TGC GCC GCC TTG TCG TTG AGG CCA A-3'
P_*CC_2324 (CCNA_02409)*	5'- AAA AAA GAA TTC GCG CCC TTC ACA AGC ATG CGA A-3'
P_*CC_2324 (CCNA_02409)*	5'- AAA AAA TCT AGA ACG GCT CCG GCG GTC GCC AGC AAC A-3'

P_*CC_2810 (CCNA_02901)*	5’- AAA AAA GAA TTC AAC CAT TAT AAT TCG GGC ACA AA-3’
P_*CC_2810 (CCNA_02901)*	5’- AAA AAA AAG CTT GTA GCC GGT CAG GCG CTG GAA-3’
P_CC_2819 (CCNA_02910)	5’- AAA AAA GAA TTC TCA GGG GCG GGT GCT GGG GCA TT-3’
P_CC_2819 (CCNA_02910)	5’- AAA AAA TCT AGA GTG GCG CCG CCT GAA ACG ACG CGA A-3’
P_*CC_2839 (CCNA_02931)*	5’- AAA AAA GAA TTC CCA AGT CCG CGA CGG CGG CGA A-3’
P_*CC_2839 (CCNA_02931)*	5’- AAA AAA TCT AGA ATC ATC TTG TCG GCC GTG CGG ACC A-3’
P_*CC_2882 (CCNA_02976)*	5’- AAA AAA GAA TTC TGG GCG CCT CCT CGG CGA CCT TAA CAA-3’
P_*CC_2882 (CCNA_02976)*	5’- AAA AAA TCT AGA AGG TCA GCC AGG GCG TGG GCG AA-3’
P_*CC_2939 (CCNA_03034)*	5’-AAA AAA GAA TTC AAT CCC CGC ACC GCA GAC CCC CAA-3’
P_*CC_2939 (CCNA_03034)*	5’-AAA AAA TCT AGA CGG CGT CAC GCT CAG ACC TTC ATG T-3’
P_*CC_3001 (CCNA_03096)*	5’-AAA AAA GAA TTC GGA CCT TGA GTC GGC CCT CAA AA-3’
P_*CC_3001 (CCNA_03096)*	5’-AAA AAA TCT AGA GCC GGA GAC CTC GAT GTC CCT TT-3’
P_*ctrA (CC_3035, CCNA_03130)*	5’-AAA AAA GAA TTC CTG CGA CGC CTG CGA CCA ATG TGT T-3’
P_*ctrA (CC_3035, CCNA_03130)*	5’-AAA AAA TCT AGA TTG ATG ACC GAC TGG GCG TGA CCC TT-3’
P_ *CC_3144 (CCNA_03246)*	5’-AAA AAA GGA TCC GAT CAT CAG GAT CGT CGC CAG GAA-3’
P_ *CC_3144 (CCNA_03246)*	5’-AAA AAA AAG CTT GGT CGC CCC GCC AGC CCT CGA TCA-3’
P_*CC_3439 (CCNA_03552)*	5’- AAA AAA GAA TTC AGA CAG TCG GCA GGC CTT GCT CCT T -3’
P_*CC_3439 (CCNA_03552)*	5’- AAA AAA TCT AGA GCG CGT TCT TGG TCG CGC CGA TCT T -3’
P_*CC_3676 (CCNA_03790)*	5’- AAA AAA GAA TTC TTG ATA GTC GCA GTC GAG CAG CTT -3’
P_*CC_3676 (CCNA_03790)*	5’- AAA AAA TCT AGA CGT CGG GCT GCA CGA ACG GCT TTT-3’
P_*CC_3689 (CCNA_03803)*	5’- AAA AAA GAA TTC AGG TGT TCA TCG AGA CCT CGA CCA A-3’
P_*CC_3689 (CCNA_03803)*	5’- AAA AAA TCT AGA CTG ACG CAC CCG CAC CGG CAG GAA-3’
P_*pleA (CC_2326, CCNA_02411)*	5’- AAA AAA AGA TCT CAG GTC TGG TCG ACG AAC TGG AA-3’
P_*pleA (CC_2326, CCNA_02411)*	5’- AAA AAA AAG CTT GAG AGG CAC GGT TTC GAC GA-3’
P_ *flaF (CC_1459, CCNA_01526)*	5’- AAA AAA CAA TTG AAG CTG TCG CTG AAG CCT GGG GAA AA-3’
P_ *flaF (CC_1459, CCNA_01526)*	5’- AAA AAA TCT AGA CCA TCG GGA GCT GGT TCT CAG GAA-3’
P_*fliX (CC_2581, CCNA_02664)*	5’- AAA AAA GAA TTC AGG AGG CGG CGA CCA GGG CGG TCA GAA-3’
P_*fliX (CC_2581, CCNA_02664)*	5’- AAA AAA TCT AGA AGG GCG ATC CGA ACC TCG CCC AGA A-3’
P_*fliQ (CC_1075, CCNA_01129)*	5’- AAA AAA GAA TTC GCG ATC CTG AAC TGC CTG GTG AAG AA-3’
P_*fliQ (CC_1075, CCNA_01129)*	5’- AAA AAA TCT AGA ATC AGC GAG CCC ATC AGC GGT AGG AA-3’
P_*NGR_a00570*	5’- AAA AAA GAA TTC CAG ATC TGC CAC CCA AGC CGA TAA-3’
P_*NGR_a00570*	5’- AAA AAA TCT AGA AAC TGA AAT ATC GAG CGT TCT CAG AA-3’
P_*NGR_a00610*	5’- AAA AAA GAA TTC GGG CTG AAG CCG CCA AAG CAG GAA-3’
P_*NGR_a00610*	5’- AAA AAA TCT AGA AAA CAG GCC AAT CAC CGC GAC AA-3’
P_*NGR_a02310*	5’- AAA AAA GAA TTC AGA CGC CCT ACA CCA TGA ACG AAA-3’
P_*NGR_a02310*	5’- AAA AAA TCT AGA GAA TGC GAC AGC GGA CAA ACC AA-3’
P_*NGR_a03530*	5’- AAA AAA GAA TTC AGC TTG AAG CTA CTT GAA GCA GTT AA-3’
P_*NGR_a03530*	5’- AAA AAA TCT AGA ATT CAT AGT CCG ATC TTT TGT GCA-3’
P_*NGR_c06240*	5’- AAA AAA CAA TTG AAG GCG ACG GTC ACG AGA GTG CCC AA-3’
P_*NGR_c06240*	5’- AAA AAA TCT AGA AGA TCA GGG TCG GCG CGT TTT CAA AA-3’

P_*NGR_c28620*	5'-AAA AAA GAA TTC GCA CCG CAG TGC TCG AAC AAC CGA TT-3'
P_*NGR_c28620*	5'-AAA AAA TCT AGA TAC CGC AAG TCG GCA ACG TTG TTC T-3'
P_*NGR_c35360*	5'-AAA AAA GAA TTC TGA TCG AGC GCC AGA CGA TCG TT-3'
P_*NGR_c35360*	5'-AAA AAA TCT AGA GAC GCC ATA GCG GAT GGC AGT CTT GTT-3'
*pilA*Cy3fw	5'-Cy3-TTCTGGATCCGGGCGAGCGC-3'
*pilA*Cy3rev	5'-Cy3-GAACTTGGTCATGACTTGGT-3'
*sciP*Cy3fw	5'-Cy3-GAAGCCTCGACCGTTGACCT-3'
*sciP*Cy3rev	5'-Cy3-GTGCGCTGCTGCTGCAACAT-3'
*ctrA*Cy3fwshort	5'-Cy3-ATGCGCGTACTGTTGATCGA-3'
*ctrA*Cy3revshort	5'-Cy3-GATTGAGGTCGAGCAGGATA-3'
*ctrA*Cy3fwlong	5'-Cy3-GTTCTTAACGCTGTAACGCC-3'
*ctrA*Cy3revlong	5'-Cy3-TCGATCAACAGTACGCGCAT-3'
pilA ChIP_F	5'-CGA CTG CAC TTA ATG GCC AG-3'
pilA ChIP_R	5'-GCC AGC ATC ACT TTC TTT GG-3'
tacA ChiP_F	5'-GTA ACC GGT TTC GCC GAC ACC GCC TAA -3'
tacA ChiP_R	5'-GTC ATC GAC GAC AAG GAC CGT TTT GGT CAT-3'
sciP ChIP_F	5'- AAC TCT TGA ATA TTA AGC GCT AAT CAT A-3'
sciP ChIP_R	5'- TGC TGC TGC AAC ATG GCT TTA CGC CTT T-3'
fliL ChIP_F	5'-ATC AAG GAG GGC CCC GAC G-3'
fliL ChIP_R	5'-TCC CGA AGG CGA AGA GGG CG-3'

Supplementary Table 1: Oligonucleotides used in this study.

SUPPLEMENTARY NOTE 1

Synthetic DNA (from dna2.0, Menlo Park, CA, USA):

mucR1^{Tn5} (5' - 3'):
ATGCCCGAATTTTCGCCATGTCGTTGGCGATCAACACGCCGCAATTGTTACAACAATTCACGAAG
CAAGTTTGATTTCAGTTTCAAACTACTTGTTTTTCTGAGGCGACCGTGTAATCCCGGATACAAGG
GGAACGGAGTTTTGAACGTGGAAGATAAAGCTACCCTAATCGAGCTTACCGCTGAAATCGTCGCT
AACTATGTGGCCAATAATTCGACGCCAGTGTCGGAACTTCCGGCCCTGATCCGGGCGACGCATGA
TGCGCTGGCCGGCATTGGCTCGCCGCCGGCGCCGACGGTTGAAGTGGTGACCAAGGCTACGCCGG
CCCAGATCCGCAAGAGCATCACGCCTGAGGCGCTGATCAGCTTCGAGGCTGACTCTTATACACAA
GTGCGGCCAGCGGCCGCTAGCGGCCGCTAG

Brucella suis BR0569 (Ros), codon optimized for *C. crescentus* (5' - 3'):
ATGGAAAACTTGGAGACGAATGACGAATCCACCGAGCTGCTGCTGAGCCTTACGGCCGACGTGGT
GGCCGCGTATGTGGGCAACAATAGCATCCGAGCCGGGGAGCTGCCGGTGCTGATCGCCGAGGTCC
ACGCGGCCTTCAAGCGCCACGTCGAGCGCGAAGAAGCGCCCGTCGTCGTTGAGAAGCCGAAGCCT
GCCGTGAACCCGAAGAAGTCGGTCCACGACGACTATATCGTCTGCCTCGAGGACGGCAAGAAGTT
CAAGTCGCTCAAGCGGCACCTGATGACCCATTACAACATGACCCCGGAGCAGTATCGCGAGAAGT
GGGATCTGGATCCCAACTACCCGATGGTCGCGCCCAACTACGCCGCTGCCCGTTCGCGCCTGGCC
AAGAAGATGGGCCTGGGCCGCAAGCCGAAAGACGCGTAA

P*_pilA(synUTR)* (5' - 3'):
GGATCCGGGCGAGCGCCAGCATCACTTTCTTTGGTCAACAAAAGACTAAAATCCACAGGCTTGCG
GCCAAGCGTCGCTTGAGAAAGTCCTTGAATCAAAAGGGCTTGGCAGCGATCGCGGAGTGCATGGT
TAAGAACAAATAACGGTAAATACAAATAAACCAAAAGAAAATCTCTGAAAACTATTCGCTGTTTA
CTGGCCATTAAGTGCAGTCGGCGAAATTGATCGTaagaaggagatatacatatgaagctt
[upper case letters show the PpilA sequence, lower case the synthetic UTR]

T5_mucR1b (5'-3'), *E. coli* T5 promoter with 2 MucR consensus motifs (underlined):
GAATTCGGATCCAATTGTGAGCGGATAACAATTACGAGCTTCATGCACAGTGAAATCATG
AAAAATTTATTTGCTTTGTGAGCGGATAACAATTATAAAGAAAATCGGGGATATCTTTTG
GGGTGTCGGGAGACGTACGGGGAATAGAATCTCTAGA

T5_mucR1b_mut1 (5'-3'), mutated base in T5 promoter underlined in bold:
GAATTCGGATCCAATTGTGAGCGGATAACAATTACGAGCTTCATGCACAGTGAAATCATG
AAAAATTTATTTGCTTTGTGAGCGGATAACAAT**G**ATAAAGAAAATCGGGGATATCTTTTG
GGGTGTCGGGAGACGTACGGGGAATAGAATCTCTAGA

T5_mucR1b_mut2 (5'-3'), mutated base in T5 promoter underlined in bold:
GAATTCGGATCCAATTGTGAGCGGATAACAATTACGAGCTTCATGCACAGTGAAATCATG
AAAAATTTATT**G**GCTTTGTGAGCGGATAACAATTATAAAGAAAATCGGGGATATCTTTTG
GGGTGTCGGGAGACGTACGGGGAATAGAATCTCTAGA

SUPPLEMENTARY DISCUSSION

Regulation of SciP targets

The SciP ChIP-Seq data showing that SciP does not efficiently bind P_{pilA} and other PleC:CtrA target promoters *in vivo* is consistent with previous ChIP-on-chip and qChIP experiments [4] that also did not reveal binding of SciP to promoters identified here as PleC:CtrA targets, with the possible exception of P_{pilA}. However, the precipitation of P_{pilA} with SciP in these qChIP experiments was inefficient compared to other sites [4]. Moreover, it is possible that the signal stems from nearby SciP binding site at *cpaB* (~770 nt distance) that is not resolved from *pilA* by these qChIP or ChIP-on-chip. Consistent with this view, an additional ChIP-seq experiment using anti-SciP antibodies that were used in the ChIP-on-chip/qChIP experiments [4] showed SciP to bind the *cpaB* promoter, but not P_{pilA}. Thus, based on these ChIP-seq analyses, we conclude SciP does not (efficiently) bind P_{pilA} and other PleC:CtrA target promoters *in vivo.*

These findings are easiest to reconcile with the model that SciP efficiently binds DNA in a sequence-specific manner and independently of CtrA *in vivo* at S-phase promoters, but not all CtrA target sites including G1-phase promoters (otherwise all CtrA-bound sites including those at the origin, at CtrA-repressed promoters such as P_{podJ}, and at the CtrA-activated promoters of G1-phase genes such as P_{pilA} should be bound by SciP). Targeting SciP to S-phase promoters (likely also promoters that are not direct CtrA targets) might serve to increase the local concentration such that CtrA is efficiently bound, dislodging RNAP from the promoter. Weak binding of SciP to CtrA at G1 promoters could still occur once SciP is expressed in early G1 phase. The accumulated

SciP would then interfere with the recruitment of RNA polymerase later in G1-phase at promoters that are not the principal targets sites of SciP *in vivo*. The consequence is that S-phase promoters are silenced first by SciP, a design that might serve to restrict promoter firing of G1-phase genes to a short window, yielding short pulse of activity to ramp up production of PilA, SciP and other G1-gene products.

SciP and FlbD targets

FlbD, a σ^{54}-dependent transcriptional activator of late (class III) flagellar promoters, was previously thought to repress all class II flagellar promoters [5], albeit this had been only validated *in vitro* and *in vivo* for P_{fliF}, but not other class II promoters [3, 6, 7, 8]. However, in ChIP-Seq experiments using polyclonal antibodies to FlbD [3] we observed FlbD at 22 target sites *in vivo* (Figure 2C, Supplementary Data 3), most of them lying within or near FlbD-activated promoters of class III genes such as *fljK*, *flaN*, *flgI*, *fljL*, *flgF* and *flgA*, and the FlbD-repressed class II promoter P_{fliF} [6, 7]. Importantly, these sites are distinct from those that SciP binds to *in vivo* (Figure 2C). Thus, FlbD and SciP target distinct class II promoters and P_{fliF} is not an *in vivo* target of SciP. It should be noted that we cannot exclude the possibility that SciP targets are also regulated by other transcription factors.

SUPPLEMENTARY METHODS

Plasmid constructions

The deletion construct for *mucR1 (CC_0933*) deletion construct was made by amplification of two fragments. The first, a 668 bp fragment flanked by a *Hin*dIII site at the 5`end and a *Bam*HI site at the 3` end, encompasses the upstream region of *mucR1* and extends 50 nt downstream of the predicted start codon. The second fragment, flanked by a *Bam*HI site at the 5`end and an *Eco*RI site at the 3'end, harboured the last 51 nt of the *mucR1* coding sequence and extended 638 nt downstream of the gene. These two fragments were triple ligated into pNPTS138 that had been restricted with *Eco*RI and *Hin*dIII. The resulting plasmid (pNPTS138-Δ*mucR1*-KO) was used to replace nt 1061526-1061998 from the *Caulobacter crescentus* NA1000 genome by a *Bam*HI site.

The deletion construct for *mucR2* (*CC_0949*) was also made by amplification of two fragments. The first, a 776 bp fragment flanked by a *Hin*dIII site at the 5`end and a *Bam*HI site at the 3` end, encompasses the upstream region of *mucR2* and extends 29 nt downstream of the predicted start codon. The second fragment, flanked by a *Bam*HI site at the 5`end and an *Eco*RI site at the 3'end, harboured the last 26 nt of the *mucR2* coding sequence and extended 514 nt downstream of the gene. These two fragments were triple ligated into pNPTS138 that had been restricted with *Eco*RI and *Hin*dIII. The resulting plasmid (pNPTS138-Δ*mucR2*-KO) was used to replace nt 1081397-1081760 from the *Caulobacter crescentus* NA1000 genome by a *Bam*HI site.

The pNPTS138-derivatives pNPTS138-hook and pNPTS138-*ctrA-ds* were used to backcross point mutations in *sciP* and *ctrA* ($sciP^{T24I}$ and $ctrA^{T170A}$). Plasmid

pNPTS138-hook was made by PCR amplifying a fragment encompassing nt 1024567-1025708 of the *C. crescentus* NA1000 genome flanked by restriction sites for *Eco*RI and *Hin*dIII, respectively, and cloning the fragment into pNPTS138. For pNPTS138-*ctrA-ds,* PCR was used to amplify nt 3278009-3278929 of the *C. crescentus* NA1000 genome flanked by restriction sites for *Hin*dIII and *Xba*I and the resulting fragment was cloned into pNPTS138 that had been cleaved with *Hin*dIII and *Spe*I.

The deletion construct for *CCNA_04006* was made by amplification of two fragments. The first, a 802 bp fragment flanked by an *Eco*RI site at the 5`end and a *Bam*HI site at the 3` end, encompasses the upstream region of *CCNA_04006* and extends 42 nt downstream of the predicted start codon. The second fragment, flanked by a *Bam*HI site at the 5`end and a *Hin*dIII site at the 3'end, harboured the last 39 nt of the *CCNA_04006* coding sequence and extended 808 nt downstream of the gene. These two fragments were triple ligated into pNPTS138 that had been restricted with *Eco*RI and *Hin*dIII. The resulting plasmid (pNPTS138-Δ*CCNA_04006*-KO) was used to replace nt 475604-476761from the *Caulobacter crescentus* NA1000 genome by a *Bam*HI site.

Plasmid pP-*flaF (CC_1459)*, pP-*fljM (CC_0792)*, pP-*sciP (CC_0903)*, pP-CC_0095, pP-*CC_0168*, pP-*CC_0420*, pP-*CC_0430*, pP-*CC_0591*, pP-*CC_0593*, pP-*CC_0845*, pP-*CC_0933* (*mucR1*), pP-*CC_0949* (*mucR2*), pP-*CC_1101*, pP-*CC_1128*, pP-*CC_1697*, pP-*CC_1982*, pP-*CC_1999*, pP-*CC_2199*, pP-*CC_2324*, pP-*CC_2810*, pP-*CC_2819*, pP-*CC_2839*, pP-*CC_2882*, pP-*CC_2939*, pP-*CC_3001*, pP-*CC_3144*, pP-*CC_3689*, pP-*ctrA*, pP-*pleA*, pP-*CC_3439*, pP-*CC_3676*, pP-*NGR_a00570*, pP-*NGR_a00610*, pP-*NGR_a02310*, pP-*NGR_a03530*, pP-*NGR_c06240*, pP-*NGR_c28620*, pP-*NGR_c35360* were made by amplifying the region of interest with primers that

introduced a suitable restriction sites to clone the PCR fragments directionally to control expression of *lacZ* in plac290 [9] using *Xba*I, *Bam*HI or *Hind*III or *Eco*RI. The oligonucleotides used for these constructions are listed in Supplementary Table 1. The pP-*pilA(synUTR)* reporter was made by ligating a synthetic fragment in which the native *pilA* untranslated leader region (UTR) was replaced by a heterologous one from *E. coli* (5'- AAGAAGGAGATATACATATGGAATTC-3', full sequence appended below).

The pP-*perP (CC_1307) -lacZ* translational reporter and the pP-*fliL (CC_3040)-*, pP-*fliF (CC_0905)-*, pP-*fliX (CC_2581)-*, pP-*flgI (CC_2582)-*, pP-*flgH (CC_2066)-*, pP-*flgE (CC_0902)-*, pP-*flgF (CC_2063)-*, pP-*flgB (CC_0953)-*, pP-*fljL (CC_1460)-* and pP*pilA (CC_2948)-lacZ* transcriptional reporters have been described previously [6, 10, 11, 12, 13, 14, 15, 16].

Wild-type *mucR1*, *mucR2* and the derivatives *mucR1*-long and *mucR1*::Tn*5* coding for MucR1 (142 residues, nt 1061622-1062050 in the NA1000 *C. crescentus* genome), MucR2 (139 residues, nt 1081367-1081786), MucR1-long (191 residues, nt 1061475- 1062050) and the truncated MucR1^{Tn5} variant (139 residues, nt 1061622 - 1061847 of *mucR1* fused to the Tn*5* reading frame for 54 nt, sequence appended below) were amplified using primers containing an *Nde*I site overlapping the start codon and an *Eco*RI site flanking the stop codon. The PCR products were subsequently cloned downstream of the vanillate-inducible promoter (P_{van}) on the high-copy number plasmid pMT335 [17](or downstream the xylose-inducible promoter P_{xyl} on the low-copy number plasmid pMT375 for *mucR1*) [17] after cleavage using *Nde*I and *Eco*RI restriction enzymes. We also cloned the *mucR* paralog CC_1356 into pMT335 using *Nde*I/*Eco*RI (171 residues, nt 1536627 -1536112 in the NA1000 genome), yielding pMT335-*CC_1356*.

The predicted TTG start codon was replaced by an ATG codon overlapping the *Nde*I site. To construct TAP-tagged variants of wild-type MucR1, MucR1(Y97C) and the truncated MucR1^{Tn5} allele, the genes were amplified using primers containing an *NdeI* site overlapping the start codon and an *EcoRI* site in the same frame (without stop codon). The PCR products were then cloned into a pMT335 derivative (pCWR512) carrying the TAP epitope cloned as an *EcoRI*/*XbaI* fragment [18].

The *mucR* homologs from *Agrobacterium tumefaciens (Atu0916), Brucella suis (BR0569*, codon optimized for *Caulobacter*, sequence shown in Supplementary Note 1), *Sinorhizobium fredii* str. NGR234 (*NGR_a00320* and *NGR_c07580)* were cloned into pMT335 using *Nde*I and *Eco*RI as described above. The resulting plasmids were used for complementation of the *C. crescentus* Δ*mucR1* Δ*mucR2* double mutant.

The pMT335-derived plasmids harboring wild-type *sciP*^{WT}, *sciP*^{T65A} or *sciP*^{T24I} were constructed by PCR amplification of *sciP* (*CC_0903*, encoded from nt 1026439-1026720 on the *C. crescentus* NA1000 genome) from NA1000, UG1278 (Δ*mucR1* Δ*mucR2 sciP*^{T65A}) and UG1277 (Δ*mucR1* Δ*mucR2 sciP*^{T24I}) and using primers containing an *Nde*I recognition sequence overlapping the start codon and an *Eco*RI site flanking the stop codon. The PCR products were subsequently cloned into pMT335, yielding pUG48 (*sciP*^{WT}), pUG47 (*sciP*^{T65A}) and pUG46 (*sciP*^{T24I}) from where the WT allele were cloned into pCWR547 using *Nde*I/*Sac*I [18], yielding the His6-SUMO-SciP expression plasmid pUG98 and the His6-SUMO-SciP(T24I) expression plasmid pUG97.

Similarly wild-type *ctrA* (nt coordinates 3279647-3278952 on the *C. crescentus* NA1000 genome) or mutant derivatives were cloned down-stream of P_{van} on pMT335 or of P_{xyl} on the high-copy number plasmid pMT464 [17] using *Nde*I and *Eco*RI-mediated

cleavage of sites overlapping the start codon and flanking the stop codon of *ctrA*, respectively.

To make pMT335-*CCNA_04006*, we amplified *CCNA_04006* (nt coordinates 475559-476800 of NA1000) by PCR using primers containing an NdeI recognition sequence overlapping the start codon and an *Eco*RI site flanking the stop codon. The PCR product was subsequently cloned into pMT335.

The His_6-SUMO-MucR1 and His_6-SUMO-MucR2 overexpression plasmids (pUG30 and pUG41, respectively) were made by liberating *mucR1* or *mucR2* from the pMT335-derived plasmids (see above) by restriction digest with *Nde*I and *Sac*I and ligating the fragment into the pET28a-derivative pCWR547 [18] from which the insert had been released by prior cleavage with *Nde*I/*Sac*I.

The His_6-MucR1 and His_6-MucR2 overexpression plasmids (pCWR350 and pUG12, respectively) were made by liberating *mucR1* or *mucR2* from the pMT335-derived plasmids (see above) following cleavage with *Nde*I and *Eco*RI and ligating the released fragment into pET28a (EMD Millipore, Billerica, MA) using the same restriction enzymes.

Plasmid pET28a-His_6-SUMO was constructed by digesting plasmid pUG30 with *Nde*I and *Nco*I and ligating the 300 bp fragment with the *Nde*I and *Nco*I cut plasmid pET28a.

ChIP-Seq analysis

Immunoprecipitated chromatin (*see Quantitative chromatin immunoprecipitation assays for details*) was used to prepare sample libraries used for deep-sequencing at Fasteris SA (Geneva, Switzerland). ChIP-Seq libraries were prepared using the DNA Sample Prep Kit (Illumina) following manufacturer instructions. Single-end run were performed on an Illumina Genome Analyzer IIx or HiSeq2000, 50 cycles were read and yielded several million reads. The single-end sequence reads stored in FastQ files were mapped against the genome of *Caulobacter crescentus* NA1000 (NC_011916) and to *Sinorhizobium fredii* NGR234 genome (NC_012587 chromosome, NC_012586 mega-plasmid pNGR234b, and NC_00914 plasmid pNGR234a) using Bowtie (http://bowtie-bio.sourceforge.net/) allowing to map reads that match only one place in the genome (option used `-q -m 1 -S`). Bowtie results were converted into SAM/BAM formats by using samtools (http://samtools.sourceforge.net/). The standard genomic position format files (BAM) were imported into SeqMonk (http://www.bioinformatics.babraham.ac.uk/projects/seqmonk/, version 0.21.0) to build sequence read profiles. The initial quantification of the sequencing data was done in SeqMonk: the genome was subdivided into 50 bp probes, and for every probe we calculated a value that represents the number of reads which occur within the probe (using the Read Count Quantitation option).

The quantitated probe list representing the genome was exported and used by a custom Perl script to compute the relative abundance for each probe in the genome from the overall reads count of each ChIP-Seq experiment. The script also calculated the average reads count and the standard deviation of the sample that are needed to establish

a cut-off value in order to discern candidate peaks from background signal. In all the cases the average reads count plus twice the standard deviation of the sample was found to be effective to discern between candidate peaks and background noise. Cytoscape software (http://www.cytoscape.org/) was used to generate the co-regulation networks from the lists of probes using the gene annotations as described below. All ChIP-Seq data was deposited in the GEO database under accession number GSE52849. This includes data sets GSM1277021 (*Cc*_CtrA_*WT*_ChIP-Seq, Supplementary Data 1 and 7), GSM1277022 (*Cc*_SciP_*WT* _ChIP-Seq; Supplementary Data 2, and used in part in Supplementary Data 8), GSM1277023 (*Cc*_FlbD_*WT* _ChIP-Seq; Supplementary Data 3), GSM1277024 (*Cc*_MucR1_*WT* _ChIP-Seq, Supplementary Data 4 and used in part in Supplementary Data 8), GSM1277025 (*Cc*_MucR2_*WT* _ChIP-Seq, Supplementary Data 5 and used in part in Supplementary Data 8), GSM1277026 (*Cc*_CtrA_Δ*pleC*_ChIP-Seq, Supplementary Data 1), GSM1277026 (*Cc*_SciP_Δ*mucR1/2*_ChIP-Seq, Supplementary Data 6), GSM1277028 (*Sf*_CtrA_ChIP-Seq, Supplementary Data 7), GSM1277029 (*Sf*_SciP_ChIP-Seq, Supplementary Data 2), GSM1277030 (*Sf*_MucR1_ChIP-Seq, Supplementary Data 4) and GSM1277031 (*Sf*_MucR2_ChIP-Seq, Supplementary Data 5).

Mis-annotation corrections

As sometimes mis-annotation errors (e.g. a peak is often annotated to the gene that is closer to it without considering the orientation of such gene) of the probes were found in the SeqMonk annotation report, in collaboration with Dr. Matteo Brilli (LBBE, University of Lyon, FR) we have developed an in-house Java (http://www.oracle.com/)

program in order to re-annotate the probes to the correct gene. Our program scans the probes list of candidate peaks, and for each probe in the list, the distance from its center to the start codon of nearby genes was calculated. A list of newly annotated probes having the maximum enrichment value in the peak, and a distance not greater than -500 and +100 from the start codon of the nearby gene(s) is generated. The new list of probes was used to retrieve 150 bp sequences centered on the probe plus the two adjacent 50bp probes on each side for consensus motif predictions. In addition, in order to improve these predictions, we represent *C. crescentus* NA1000 and *S. fredii* NGR234 intergenic sequences as a seventh-order Markov model calculated using the intergenic sequences extracted from the two genomes.

The program resolves three possible annotation errors created by SeqMonk. When the probe is positioned in the intergenic region of two adjacent genes on the same DNA strand, SeqMonk often associates the probe to the closest gene without considering its orientation. In this case, the program does not consider the gene(s) upstream the selected probe and assigns the probe to the downstream gene if the distance from the center of the probe is not greater than 500 bp [19, 20]. In the second scenario, a probe might lie in the intergenic region of two divergent genes (e.g. the genes are on different DNA strands). In this case, the program assigns the probe to the gene when the distance to the start codon does not exceed 500 bp. In case both genes are less than 500 bp, the probe is assigned to both genes because no predictions can be made on which gene the binding site regulates. Finally, when the probe lies within the coding sequence of a gene, the probe is assigned to this gene, provided that the distance from the probe is less than 100 bp from the start codon. If the distance exceeds 100 bp, the probe is assigned to a nearby gene provided

that the aforementioned criteria are fulfilled. All probes that fulfill these criteria are given association(s) to coding genes, but the "ANNO" list in the Supplementary Data 1-9 reports only the probe with the highest relative abundance. Probes that cannot be linked to a coding gene are placed in a separate list ("NOANNO" in the Supplementary Data 1-9). We also checked if our analysis method is applicable to other ChIP-Seq available on the GEO database by re-analysis of a heterologous ChIP-Seq data of mycobacterial origin (accession GSE52849) [21]. Specifically we considered the SRA568027 dataset that corresponds to the RNA polymerase (RNAP) ChIP-Seq performed during the exponential phase in *Mycobacterium tuberculosis* H37Rv. The SRA568027 dataset was converted in FastQ format using sratoolkit.2.3.4-2 and reads were mapped to the genome of *M. tuberculosis* H37Rv as described in Supplementary Methods *"ChIP-Seq analysis"*. We compared the ANNO probes file from our analysis to the corresponding enrichment values for RNAP ChIP-seq reported in Supplementary Table 4 in Uplekar et al [21]. We were able to identify more than 60% of the targets reported to be significantly enriched Uplekar et al [21]. The file reporting the results of our comparison it is enclosed in Supplementary Data 9).

Consensus motif predictions

The MEME [19, 20] motif finding tool were run on the set of 150 bp sequences retrieved from the two genomes in order to identify the most over-represented motif. In computational searches for CtrA, MucR1 and MucR2 boxes, the likelihood that each sequence contained a CtrA, MucR1 or MucR2 box was compared with the likelihood that

it was a typical *Caulobacter* intergenic sequence (represented using a seventh-order Markov model).

For the CtrA^{Cc} ChIP-seq dataset, MEME runs were launched on the whole set of target sequences that made the cut-off described above. After MEME runs we retained only motifs with an *E*-value of $\geq 1.00 \bullet e^{-06}$, in this way we filtered out 88/280 sequences. These 88 sequences were used to build the PSSM describing the consensus motif and for generate the Sequence logo (http://weblogo.berkeley.edu/). In the filtered list we were able to map the motif in genes for which there is experimental (biochemical) evidence. In the case of CtrA^{Cc}, there is experimental [2, 22, 23, 24, 25, 26, 27, 28, 29, 30] or [25, 28, 31, 32] information on its regulon. Therefore, it was possible to evaluate motifs on previous datasets and ours. Among the 88 sequences 21 were used to construct the *lacZ* transcriptional reporter.

Consensus motif prediction on the CtrA^{Sf} ChIP-seq dataset was made on the top ranked sequences hailing from chromosome and the two plasmids pNGR234a, pNGR234b. 54/127 sites were retained having an *E*-value of $\geq 1.00 \bullet e^{-06}$; among these 54 sequences 4 were cloned in plac290 and promoter activity tested.

In our attempt to define a consensus sequence for the MucR1 and MucR2 DNA binding proteins in both *C. crescentus* and *S. fredii*, we decided to use as training set in MEME runs only the top ranked sequences of MucR1 and MucR2 datasets. Also in this case we retained only motifs having an *E*-value of $\geq 1.00 \bullet e^{-06}$ to describe the consensus.

We filtered out using this cut off, 50/179 and 38/276 sequences for each MucR1^{Cc} and MucR2^{Cc} dataset respectively. 19/50 and 9/38, MucR1^{Cc} and MucR2^{Cc} consensus sequences were cloned into plac290 for *lacZ* transcriptional reporter experiments.

For MucR1^{Sf} and MucR2^{Sf} we used as training set for MEME scans the top ranked sequences coming from both chromosome and plasmid ChIP-seq data. In MucR1^{Sf}, scanned sequences 71/282 have a motif with an *E*-value of $\geq 1.00 \bullet e^{-06}$, while in MucR2^{Sf} only 61/259 have a motif that fulfill the $1.00 \bullet e^{-06}$ cut-off. Among the sequences filtered out using this cut-off, 5 sequences were selected for *lacZ* reporter constructions in plac290.

In order to predict a SciP consensus motif (sheet 5 in Supplementary Data 2), we took advantage of three different ChIP-Seq data sets we performed with three different antibodies. A first data set was generated by using our custom SciP antibody, the other two data sets were generated by using custom-made antibodies described previously (accession GSE52849) [4,2]. The three dataset were analyzed as described above, and a list of candidate peaks was generated for each of them.

The three candidate peak lists were used to extract peaks that are common to three ChIP-Seq in order to compile a "high confidence" target set. The common targets list was compared to the SciP target sites precipitated more efficiently from Δ*mucR1* Δ*mucR2* double mutant chromatin versus NA1000 (*WT*) chromatin (Supplementary Data 6). By applying this strategy we were able to retain only those targets that are highly likely to be SciP targets *in vivo*. This list of common targets was used to extract the nucleotide sequences of their corresponding probes and the two adjacent 50-bp probes upstream and downstream. The resulting 150 bp sequences were scanned by MEME to identify a consensus motif, (G/A)TTAACCAT(A/G), for SciP (position probability matrix shown in Supplementary Data 2, sheet 5). MEME analysis was performed with the following parameters -dna -mod zoops -nmotifs 3 -bfile BKG_MARKOV7_CCRE.txt -nomatrim -

revcomp -maxsize 1000000 -maxiter 1000, and it was implemented by using a 7^{th} order Markov Model describing nucleotides sequences in *C. crescentus* DNA.

SUPPLEMENTARY REFERENCES

1. Domian IJ, Quon KC, Shapiro L. Cell type-specific phosphorylation and proteolysis of a transcriptional regulator controls the G1-to-S transition in a bacterial cell cycle. *Cell* **90**, 415-424 (1997).

2. Gora KG, Tsokos CG, Chen YE, Srinivasan BS, Perchuk BS, Laub MT. A cell-type-specific protein-protein interaction modulates transcriptional activity of a master regulator in *Caulobacter crescentus*. *Mol Cell* **39**, 455-467 (2010).

3. Davis NJ, Viollier PH. Probing flagellar promoter occupancy in wild-type and mutant *Caulobacter crescentus* by chromatin immunoprecipitation. *FEMS Microbiol Lett* **319**, 146-152 (2011).

4. Tan MH, Kozdon JB, Shen X, Shapiro L, McAdams HH. An essential transcription factor, SciP, enhances robustness of *Caulobacter* cell cycle regulation. *Proc Natl Acad Sci U S A* **107**, 18985-18990 (2010).

5. Wu J, Newton A. Regulation of the *Caulobacter* flagellar gene hierarchy; not just for motility. *Mol Microbiol* **24**, 233-239. (1997).

6. Wingrove JA, Gober JW. A sigma 54 transcriptional activator also functions as a pole-specific repressor in *Caulobacter*. *Genes Dev* **8**, 1839-1852 (1994).

7. Benson AK, Ramakrishnan G, Ohta N, Feng J, Ninfa AJ, Newton A. The *Caulobacter crescentus* FlbD protein acts at ftr sequence elements both to activate and to repress transcription of cell cycle-regulated flagellar genes. *Proc Natl Acad Sci U S A* **91**, 4989-4993. (1994).

8. Benson AK, Wu J, Newton A. The role of FlbD in regulation of flagellar gene transcription in *Caulobacter crescentus*. *Res Microbiol* **145**, 420-430. (1994).

9. Gober JW, Shapiro L. A developmentally regulated *Caulobacter* flagellar promoter is activated by 3' enhancer and IHF binding elements. *Mol Biol Cell* **3**, 913-926 (1992).

10. Chen JC, Hottes AK, McAdams HH, McGrath PT, Viollier PH, Shapiro L. Cytokinesis signals truncation of the PodJ polarity factor by a cell cycle-regulated protease. *EMBO J* **25**, 377-386 (2006).

11. Skerker JM, Shapiro L. Identification and cell cycle control of a novel pilus system in *Caulobacter crescentus*. *Embo J* **19**, 3223-3234 (2000).

12. Boyd CH, Gober JW. Temporal regulation of genes encoding the flagellar proximal rod in *Caulobacter crescentus*. *J Bacteriol* **183**, 725-735 (2001).

13. Mangan EK, Bartamian M, Gober JW. A mutation that uncouples flagellum assembly from transcription alters the temporal pattern of flagellar gene expression in *Caulobacter crescentus*. *J Bacteriol* **177**, 3176-3184 (1995).

14. Mohr CD, Jenal U, Shapiro L. Flagellar assembly in *Caulobacter crescentus*: a basal body P-ring null mutation affects stability of the L-ring protein. *J Bacteriol* **178**, 675-682 (1996).

15. Mohr CD, MacKichan JK, Shapiro L. A membrane-associated protein, FliX, is required for an early step in *Caulobacter* flagellar assembly. *J Bacteriol* **180**, 2175-2185 (1998).

16. Dingwall A, Garman JD, Shapiro L. Organization and ordered expression of *Caulobacter* genes encoding flagellar basal body rod and ring proteins. *J Mol Biol* **228**, 1147-1162 (1992).

17. Thanbichler M, Iniesta AA, Shapiro L. A comprehensive set of plasmids for vanillate- and xylose-inducible gene expression in *Caulobacter crescentus*. *Nucleic Acids Res* **35**, e137 (2007).

18. Radhakrishnan SK, Pritchard S, Viollier PH. Coupling prokaryotic cell fate and division control with a bifunctional and oscillating oxidoreductase homolog. *Dev Cell* **18**, 90-101 (2010).

19. Bailey TL, Elkan C. The value of prior knowledge in discovering motifs with MEME. *Proceedings / International Conference on Intelligent Systems for Molecular Biology ; ISMB International Conference on Intelligent Systems for Molecular Biology* **3**, 21-29 (1995).

20. Bailey TL, Williams N, Misleh C, Li WW. MEME: discovering and analyzing DNA and protein sequence motifs. *Nucleic Acids Res* **34**, W369-373 (2006).

21. Uplekar S, Rougemont J, Cole ST, Sala C. High-resolution transcriptome and genome-wide dynamics of RNA polymerase and NusA in *Mycobacterium tuberculosis*. *Nucleic Acids Res* **41**, 961-977 (2013).

22. Biondi EG, *et al.* Regulation of the bacterial cell cycle by an integrated genetic circuit. *Nature* **444**, 899-904 (2006).

23. Modell JW, Hopkins AC, Laub MT. A DNA damage checkpoint in *Caulobacter crescentus* inhibits cell division through a direct interaction with FtsW. *Genes Dev* **25**, 1328-1343 (2011).

24. Jonas K, Chen YE, Laub MT. Modularity of the bacterial cell cycle enables independent spatial and temporal control of DNA replication. *Curr Biol* **21**, 1092-1101 (2011).

25. Laub MT, Chen SL, Shapiro L, McAdams HH. Genes directly controlled by CtrA, a master regulator of the *Caulobacter* cell cycle. *Proc Natl Acad Sci U S A* **99**, 4632-4637 (2002).

26. Holtzendorff J, *et al.* Oscillating global regulators control the genetic circuit driving a bacterial cell cycle. *Science* **304**, 983-987 (2004).

27. Iniesta AA, McGrath PT, Reisenauer A, McAdams HH, Shapiro L. A phospho-signaling pathway controls the localization and activity of a protease complex critical for bacterial cell cycle progression. *Proc Natl Acad Sci U S A* **103**, 10935-10940 (2006).

28. Spencer W, Siam R, Ouimet MC, Bastedo DP, Marczynski GT. CtrA, a global response regulator, uses a distinct second category of weak DNA binding sites for cell cycle transcription control in *Caulobacter crescentus*. *J Bacteriol* **191**, 5458-5470 (2009).

29. Jenal U, Galperin MY. Single domain response regulators: molecular switches with emerging roles in cell organization and dynamics. *Curr Opin Microbiol*, (2009).

30. Angelastro PS, Sliusarenko O, Jacobs-Wagner C. Polar localization of the CckA histidine kinase and cell cycle periodicity of the essential master regulator CtrA in *Caulobacter crescentus*. *J Bacteriol* **192**, 539-552 (2010).

31. Laub MT, McAdams HH, Feldblyum T, Fraser CM, Shapiro L. Global analysis of the genetic network controlling a bacterial cell cycle. *Science* **290**, 2144-2148 (2000).

32. Brilli M, *et al.* The diversity and evolution of cell cycle regulation in alpha-proteobacteria: a comparative genomic analysis. *BMC Syst Biol* **4**, 52 (2010).